Morin Transition Temperature of α-Hematite using Mössbauer Spectroscopy

T.J. Wertheim, E.J. Lagendijk

May 4, 2026

Abstract

Using Mössbauer spectroscopy the Morin transition temperature of α-hematite was found. Using a γ-radiating source together with a transducer and a γ-detector, a Morin transition was observed at a temperature of $T_{Morin} = 238$ K. This temperature is believed to be due to incorrect cooling of the sample, causing the shift to incorrectly appear at values when it should not have been observed.

Contents

1 Introduction **2**

2 Theory **3**
2.1 Newton's Nuclear Third Law 3
2.2 Nuclear Resonance 3
2.3 Quantum mechanics 3
2.4 Relativistic Doppler Effects 4
2.5 Hematite and its Morin Transition 4

3 Method **5**
3.1 Experimental setup 5
3.2 Measurement Procedure 6

4 Results **6**

5 Discussion **9**
5.1 Quadrupole split outlier 9
5.2 Data analysis and future research 9

6 Conclusion **9**

7 Bibliography **10**

1 Introduction

The Mössbauer effect is a phenomenon that makes use of recoil-free emission and absorption, as well as nuclear resonance, in order to find material properties of certain compounds. This proves to be to be extremely useful in fields such as cosmology, where matter cannot be transported to a laboratory for research and must be analyzed from a distance. Mössbauer spectroscopy is a pioneering method to analyze the surface of Mars and discover the compounds that the surface is made of, without requiring the samples to be transported to to Earth for further analysis [1]. Specifically, NASA has used Mössbauer spectroscopy on rovers such as Spirit and Oppertunity to investigate the concentration of α -hematite on the surface, which could determine the favorability of life on Mars in the past [2].

This research paper was conducted as part of the Research Practicum subject at TU Delft and its purpose is to learn more about how this method of α-hematite concentration analysis is done using Mössbauer spectroscopy. This is done by finding the Morin transition temperature, a temperature at which the compound changes from antiferromagnetic to ferromagnetic. The literature values place the Morin transition temperature at $T_{Morin} = 260$ K [3].

2 Theory

2.1 Newton's Nuclear Third Law

Newton's third law requires each reaction to have an equal and opposite reaction. A nucleus that drops from a high energy state to a lower state emits a photon, meaning this nucleus must experience an equal force to contradict the emission of the photon. Since the momentum of the photon and the recoil is identical but opposite (defined by Newton's third law), an equation can be easily derived for the recoil energy E_{recoil} of a nucleus. Using the following two equations for kinetic energy and momentum respectively:

$$E_{kin} = \frac{1}{2}mv^2 \qquad (1) \qquad\qquad p = mv \qquad (2)$$

With M and v being the mass and velocity of the nucleus respectively. The energy can be rewritten as:

$$E_{recoil} = \frac{p_\gamma^2}{2m} = \frac{p_{recoil}^2}{2m} = \frac{E_\gamma^2}{mc^2} \qquad (3)$$

Taking into account that photons travel at the speed of light, meaning $v_\gamma = c$. Given the conservation of energy, this recoil energy must therefore come from the original gap energy E_{gap}, meaning the recoil energy could conversely be written as:

$$E_{recoil} = E_{gap} - E_\gamma \qquad (4)$$

2.2 Nuclear Resonance

One could imagine a scenario in which a nucleus drops from a higher energy state to a lower one, therefore emitting a photon which causes a neighboring nucleus to consequently absorb this photon and thus jump to the higher state mentioned above. This domino-like effect is called nuclear resonance. However, this is only possible if the absorbed photon has the exact energy necessary to jump to the higher energy state and because a tiny but significant amount of the original energy E_{gap} being spent on the recoil E_{recoil}, the energy left in the photon is always slightly less than needed and therefore will not produce nuclear resonance [4].

2.3 Quantum mechanics

Nuclear resonance is therefore only possible if the recoil energy is zero. In other words, $E_\gamma = E_{gap}$. Classically this is impossible, as the act of emitting a photon with a certain momentum must (following Newton's 3rd law) produce an identical momentum in the opposite direction. A way to circumvent this however is by making use of quantum mechanics and molecular lattices.

In a lattice, E_{recoil} is transferred as a vibration that moves throughout the lattice, called a phonon. Since phonons are quantized, there exists a certain minimum energy $E_{ph,min}$ for phonons. A phonon with an energy below this level can not exist. If a nucleus produces a recoil energy below this threshold, a classical paradox arises. If no phonon is produced, this recoil energy is spontaneously destroyed. If a minimum energy phonon is produced however, more energy is spontaneously created. Both these situations violate the conservation of energy and thus are not the correct explanation.

In quantum mechanics, in this scenario a phonon may be created with the minimum energy or a phonon may not be created at all. Both these situations happen simultaneously with certain probabilities to collapse into one of the given situations dependent on the energy of the original recoil. Since the energy only contributes to the probability of existing and not the final energy of the phonon, this is a way to create phonons with a constant energy that are independent of the recoil energy that created them.

2.4 Relativistic Doppler Effects

Due to hyperfine interactions, the true energy difference is slightly off. To combat this to allow for nuclear resonance, the photon emitter can be moved towards the sample at a speed v. Relativistically, the energy of a photon E_γ is defined by:

$$\frac{E_\gamma(v)}{E_{gap}} = \sqrt{\frac{1+\frac{v}{c}}{1-\frac{v}{c}}} \tag{5}$$

By varying this speed the energy of the emitted photons can be varied and a spectrum made of the number of counts detected by a γ-detector plotted against the Doppler speed v. Since nuclear resonance will cause certain energies (and therefore speeds) to be absorbed, they show up as dips. This leaves an identifiable fingerprint from which the material in question can be identified.

2.5 Hematite and its Morin Transition

Hematite is a compound with the formula Fe_2O_3. Hematite is antiferromagnetic under a certain temperature, called the Morin temperature. Antiferromagnetic refers to how the particles order themselves in the compound. Antiferromagnetic materials contain atoms that are antiparallel to the magnetic moment of the atom, which leads to no net magnetic field. This is the case of α-hematite under the Morin temperature. Above this temperature, the atoms are slightly slanted. Since the slant causes an imperfect antiparallel alignment, this causes a small magnetic field to be created, something often referred to as weak ferromagnetism [5].

3 Method

3.1 Experimental setup

. The experimental setup used to measure Mössbauer spectroscopy consists of a transducer, a radioactive source that emits gamma particles, a sample that absorbs the gamma particles and a γ-detector.

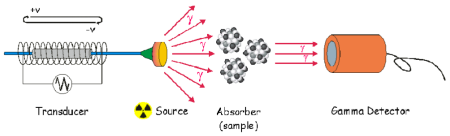


Figure 1: Experimental setup [6]

The radioactive source used in the experiment was ^{57}Co which decays to ^{57}Fe after electron capture.

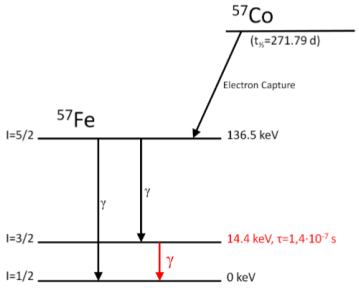


Figure 2: The decay-scheme of ^{57}Co

The isotope ^{57}Fe, which is in an excited state, decays to its ground state by emitting a 14.4 keV gamma particle.

The transducer will move the source with a velocity range of $-10mm/s$ to $10mm/s$ to tune the energy of the gamma particles. Here the Doppler shift is used in order to adjust the wavelength of the gamma particles which will cause a difference in energy. After this the gamma particles will get absorbed by the sample due to the Mössbauer effect [7].

The gamma particles that are not absorbed by the sample will pass through the detector. The detector is a proportional counter which is a tube filled with gas in which a thin conducting wire is mounted. The high voltage supply will cause a electric field inside the tube. The incoming particles will ionize the gas molecules. The electrons will then accelerate to the positive charged wire and will ionize more molecules on their way. This causes a chain reaction. The charge on the wire will be measured, and the pulse height depends on the energy

of the ionizing particles. To get the pulse voltage to a measurable amplitude, an amplifier will be used.

Lastly, the electronics contain a function generator for the transducer and it will also count the number of pulses. During one period of the function, the electronics will go through 1024 measurement channels. If a gamma particle is measured the channel were the electronics are in will increase with one. At the end, every channel contains the count belonging to a certain Doppler velocity.

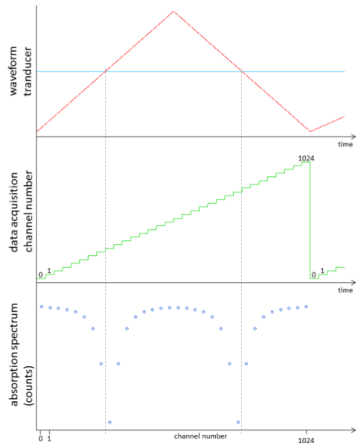


Figure 3: The top graph the velocity signal, the middle graph shows how the data is acquired and the bottom graph shows the Mössbauer spectrum.

To acquire the Mössbauer spectrum as shown in figure 3 a calibration must be done by measuring standard absorbers with known position of peaks. This can convert the x-axis into a energy scale (mm/s). This calibration was done with SNP (sodium nitroprusside).

3.2 Measurement Procedure

For the measurement procedure, the sample was cooled below room temperature using liquid nitrogen. Temperature-dependent measurements were conducted within the range of 173 K to 293 K. The initial measurement was performed at 173 K, followed by incremental temperature increases of 20 K per step until the maximum temperature of 293 K was reached. Each measurement had a minimum measurement time of 6 hours.

4 Results

Figure 4 shows the Morin transition at 258 K and the green line shows the shift from the measurement at 238 K to the measurement at 278 K. A table with all the measurement values at different temperatures is indicated in the appendix.

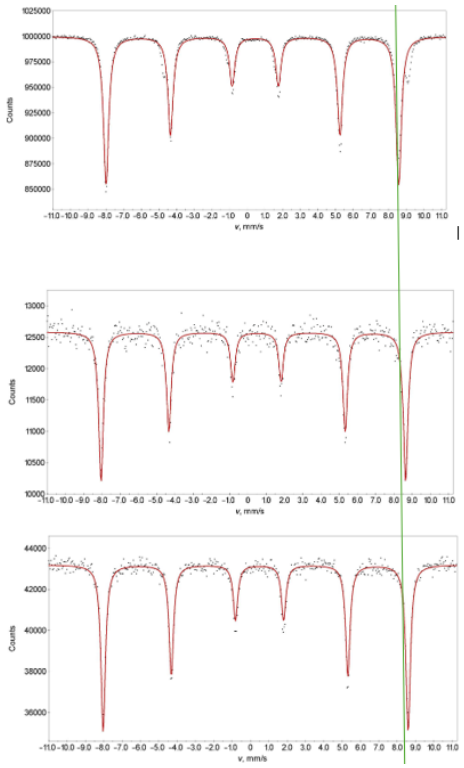


Figure 4: The top graph showcases the measurement at 238 K, the middle at 258K and the bottom at 278K

In all cases, an electric field gradient as well as an external magnetic field are present. This causes the 6 peaks to occur in each scenario, 4 resulting from the electric quadropole splitting and 2 due to the magnetic hyperfine splitting.

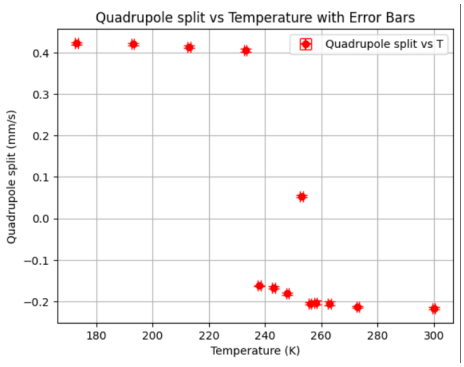


Figure 5: Quadrupole split in mm/s against the temperature in K with errorbars.

Looking at the graph in figure 5, it clearly showcases a change in the quadrupole split at 238 K. A declaration for this sudden change is the change of the anti-ferromagnetic state to the ferromagnetic state.

In figure 5 there is a data point between the two constant values, at a temperature of $T = 253$ K. More on the reasons of this in the discussion.

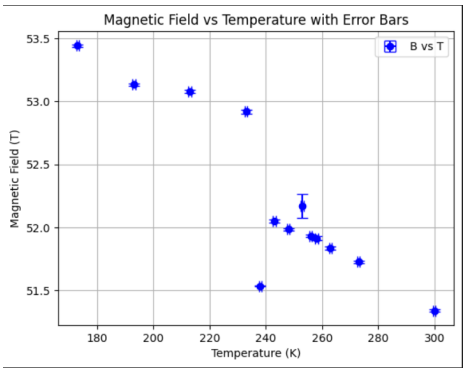


Figure 6: Magnetic field in T plotted against the temperature in K with error-bars.

The same conclusion can be made of figure 6 where the sudden change in the magnetic field is shown at 238 K as well.

The magnetic field decreases as the temperature increases. This is because the higher the temperature, the more sporadically the atoms move, causing the aligned magnetic moment of the atoms to become less and less aligned, resulting in a less strong magnetic field. The Morin temperature causes a sharp drop in magnetic field strength due to its effect of the antiparallel alignment of the atoms, dropping the overall net field.

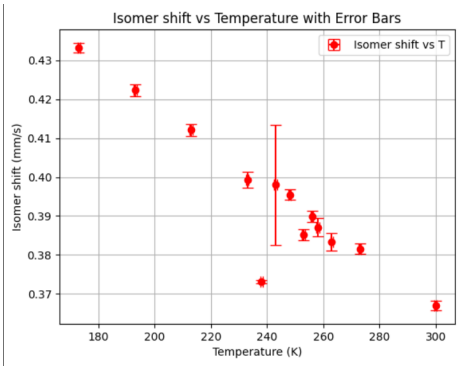


Figure 7: The isomer shift is shown in mm/s against the temperature

The last figure indicates a decrease in isomeric shift as the temperature of

the samples increases. A decrease in the isomeric shift indicates a higher electron density at the nucleus. The higher temperature will expand the lattice structure, which changes the electron density.

Since the isometric shift revolves around the Coulomb interactions and electric forces and the Morin transition alters the magnetic forces, the Morin transition should not have much effect on the isometric shift. This is also what can be seen in figure 7; the trend continues linearly downwards through the Morin temperature of 228 K.

5 Discussion

5.1 Quadrupole split outlier

In figure 5 there is an outlying data point at $T = 253$ K. We believe this to be due to the increments of temperature increase. Starting from 173 K, we measured in increments of 20 K. This means that we warmed the sample 253 K, after which we measured a change and decided to cool it off to a lower temperature to further investigate the interval. Following our chronological order of measurements, we see from figure 5 that the QS consistently drops, as the outlier was measured before the points just below it at temperatures $T = 238$ K, $T = 241$ K and $T = 243$ K. Due to this 'early' QS drop, we believe it partially transitioned making the QS irreversible afterwards, which is not uncommon for some forms of α-hematite. Our sample going through an early Morin transition would also explain the temperature value differing from the literature value of 260 K, however depending on the form of α-hematite, this value can range from 241-260 K [8]. With 253 K being exactly in this range, this would furthermore explain why an early transition might have taken place.

5.2 Data analysis and future research

The data shows the Morin transition occur at a temperature of $T_{Morin} = 238$ K. This can be seen by the shift of the top graph in figure 4, as well as the sudden jumps of the quadrupole split and magnetic field strength in figures 5 and 6 respectively. Future research could be improved by using the literature value of $T_{Morin} = 260$ K as a benchmark to work towards, as consistently cooling and warming the sample could result in unwanted effects that could potentially jeopardize the research. Furthermore the type of α-hematite can be researched in order to find its exact Morin transition temperature.

6 Conclusion

The Morin transition was observed to occur at a temperature of $T_{Morin} = 238$ K. This is supported by a shift in the Mössbauer transition spectrum and a drop in values of the quadrupole split and magnetic field strength, all at a temperature of

$T = 238$ K. Our found value differs from the literature value range of $T_{Morin,lit} = 241 - 260$ K. We believe this to be due to an early transition during the heating of the sample to the temperature $T = 253$ K, which can be seen as an outlier in the values of the quadrupole split. To improve, future research could use the literature value as a benchmark to work towards in order to limit the size of interval jumps and the amount of heating and cooling necessary.

7 Bibliography

[1] De Souza Jr., P. A., Morris, R. V., Klingelhöfer, G., Athena Science Team. (n.d.). ANALYSIS OF MÖSSBAUER DATA FROM MARS: A DATABASE AND ARTIFICIAL NEURAL NETWORK FOR IDENTIFICATION OF IRON-BEARING PHASES. Sixth International Conference on Mars, 3143. https://www.lpi.usra.edu/meetings/sixthn

[2] Davis, P., Davis, P. (2024, November 3). Mars Exploration Rovers: Spirit and Opportunity - NASA Science. NASA Science. https://science.nasa.gov/mission/mars-exploration-rovers-spirit-and-opportunity/

[3] Woods, G. T.; Callcott, T. A. (2000). "X-ray magnetic linear dichroism in -Fe2O3". APS March Meeting Abstracts. Bibcode:2000APS..MARA24005W.

[4] N. van Dijk, M.P. Steenvoorden, A.I Dugulan (n.d.). Mössbauer spectroscopy. TUD-RID, rev. 28-10-2024

[5] Saini, R. K., Bagri, L. P., Bajpai, A. K., Mishra, A. (2018). Responsive polymer nanoparticles for drug delivery applications. In Elsevier eBooks (pp. 289–320). https://doi.org/10.1016/b978-0-08-101997-9.00015-1

[6] Steenvoorden, M. (n.d.). Description of a Mössbauer-spectrometer. TUD-RID

[7] Gopal, E. S. R., Sinha, A. P. B. (1971). Thermoelectric power of simple metals at high temperatures. Journal of Low Temperature Physics, 4(5), 467–478. https://doi.org/10.1007/BF02058947

[8] Özdemir, Ö., Dunlop, D. J., Berquó, T. S. (2008). Morin transition in hematite: Size dependence and thermal hysteresis. Geochemistry Geophysics Geosystems, 9(10). https://doi.org/10.1029/2008gc002110

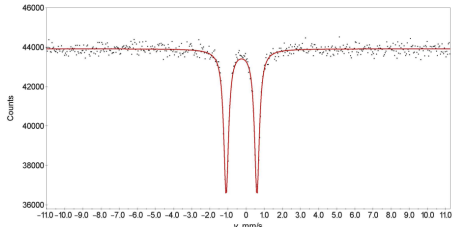


Figure 8: The calibration with sodium nitroprusside

T(K)	B(T)	u(B)(T)	$QS_p(mm/s)$	u(QS_p)(mm/s)	IS(mm/s)	u(IS)(mm/s)
173	53.440	0.024	0.422	0.008	0.433	0.003
193	53.132	0.032	0.420	0.009	0.422	0.005
213	53.077	0.032	0.414	0.004	0.412	0.005
233	52.917	0.042	0.406	0.002	0.399	0.006
238	51.537	0.007	-0.162	0.009	0.373	0.001
243	52.050	0.032	-0.166	0.009	0.398	0.045
248	51.985	0.030	-0.181	0.009	0.395	0.004
253	52.172	0.028	0.053	0.009	0.385	0.004
256	51.934	0.029	-0.205	0.015	0.390	0.004
258	51.915	0.041	-0.203	0.012	0.387	0.008
263	51.836	0.045	-0.205	0.008	0.383	0.006
273	51.728	0.027	-0.214	0.008	0.382	0.004
300	51.342	0.024	-0.216	0.009	0.367	0.003

Table 1: Table with all the measurement values at 13 different temperatures